Arch. Metall. Mater. **63** (2018), 4, 2001-2007

DOI: 10.24425/amm.2018.125136

O. CZYŻ*#, J. KUSIŃSKI*, A. RADZISZEWSKA*, R. OSTROWSKI**,
J. MORGIEL***, J. KANAK****, M. KĄC*****

MODIFICATION OF THE STRUCTURE AND PROPERTIES OF FeSiB AMORPHOUS RIBBON BY INTERFERENCE PULSED LASER HEATING

Paper describes the results of $Fe_{80}Si_{11}B_9$ amorphous ribbon investigation after pulsed laser interference heating and conventional annealing. As a result of interference heating periodically placed laser heated microareas were obtained. Structure characterisation by scanning and transmission electron microscopy showed in case of laser heated samples presence of crystalline nanostructure in amorphous matrix. Microscopy observations showed significant difference in material structure after laser heating – nanograin structure, and material after annealing – dendritic structure. Magnetic force microscopy investigation showed expanded magnetic structure in laser heated microareas, while amorphous matrix did not give magnetic signal. Change of magnetic properties was examined by magnetic hysteresis loop measurement, which showed that the laser heating did not have a significant influence on soft magnetic properties.

Keywords: Laser heating, FeSiB, Crystallization, Magnetic properties, Structure

1. Introduction

Pulsed laser interference heating (PLIH) process is based on interference at least two laser beam on sample surface [1]. Laser beam affect and create interference image (line or dots) at sample surface. This very precise technique allows to create periodically placed laser heated microareas/dots in which modification of structure and properties occurs [1-4]. Production of periodic nanostructures, uniformly distributed over large areas, makes the PLIH a fast developing tool for investigations of numerous technological processes [1].

Iron based amorphous ribbons are characterized by very soft magnetic properties [5]. Its low coercivity with high saturation magnetization, connected with high yield strength and good corrosion resistance, make this material one of extensively studied since they were invented [5-8]. Since metallic glasses are kinetically metastable materials a detailed understanding of their crystallization process is required. A suitable heat treatment, which leads amorphous material to partial crystallization, provides in some cases an improvement in properties [6]. Also chemical composition regulations can influence properties of these alloys [5,6,9].

Application energy of laser beam to amorphous ribbon heat treatment can force structure and properties changes [3,10,11]. Laser treatment is characterized by rapid heating and cooling rates what allow to achieve desired temperature. High nucleation rates occur that in turn aid in restricting the grain growth [10]. Katakam et al. [10] have shown that magnetic properties received after laser heating are much better then after conventional furnace annealing so together with short processing time and possibility to easy control the structure evaluation by selecting laser heating parameters, make laser treatment the most promising process for amorphous alloys crystallization. Moreover, application of PLIH process may provide, at the same time, crystallization in thousands microareas/dots, what allows to form two-dimensional micro-islands of laser crystallized material, periodically placed in amorphous matrix. Indeed, as results one can obtained the desired structure and properties [3,10,11].

The present work is focused on surface and microstructure evaluation, correlated with magnetic properties, of amorphous of FeSiB ribbons subject to the pulsed laser interference heating and conventional annealing.

2. Experimental procedure

The alloy in the form of a $Fe_{80}Si_{11}B_9$ amorphous 30 μm thick and 25 mm wide ribbon was investigated. Pulsed laser interference heating was performed by Nd:YAG laser in TEM_{00} mode with wavelength 1064 nm, frequency 1 Hz, and pulse time

* AGH UNIVERSITY OF SCIENCE AND TECHNOLOGY, FACULTY OF METALS ENGINEERING AND INDUSTRIAL COMPUTER SCIENCE, AL. MICKIEWICZA 30, 30-059 KRAKÓW, POLAND
** MILITARY UNIVERSITY OF TECHNOLOGY, INSTITUTE OF OPTOELECTRONICS, 2 GEN. S. KALISKIEGO STR., 00-908 WARSAW, POLAND
*** INSTITUTE OF METALLURGY AND MATERIALS SCIENCE, POLISH ACADEMY OF SCIENCES, 25 REYMONT STR., 30-059 CRACOW, POLAND
**** AGH UNIVERSITY OF SCIENCE AND TECHNOLOGY, FACULTY OF COMPUTER SCIENCE, ELECTRONICS AND TELECOMMUNICATIONS, AL. MICKIEWICZA 30, 30-059 KRAKÓW, POLAND
***** INSTITUTE OF NUCLEAR PHYSICS, POLISH ACADEMY OF SCIENCES, PL-31342 KRAKOW

Corresponding author: olafczyz@agh.edu.pl

of 8 ns. Laser heating was performed in pulsed mode. Single shot energy was changed from 120 to 480 mJ and also number of shots was changed from 1 to 500. Interference illumination field on sample surface was realized by a quartz tetrahedral prism with an apex angle of 172°. During conventional crystallization samples were heated to 600°C at 20°C/min rate and slowly cooled down in an argon atmosphere. Following thermal treatments the surfaces were investigated by scanning electron microscopy (SEM): FEI Inspect S50 instrument, transmission electron microscopy (TEM): JEOL JEM 200 CX and Tecnai G2 F20 instruments and atomic forces microscopy (AFM): Veeco Dimension® Icon™ SPM instrument at magnetic forces mode (MFM) microscopy. TEM samples were 3 mm disc excised parallel to the heated surface prepared by electro-polishing. Cross sections from laser heated area were prepared by focus ion beam (FIB) technique using FEI Quanta 3D. Magnetic properties of amorphous and laser modified samples were measured using a superconducting quantum interference device: (SQUID) magnetometer Quantum Design, MPMS, by applying an external field up to 4 T in the plane of the samples. Magnetic moment was determined with an accuracy of 2% or better.

3. Results and discussion

3.1. Material structure

Laser interference heating of amorphous ribbons produces periodically placed laser heated microareas. Figures 1-2 shows samples after interference irradiation with different laser beam energy (Fig. 1) and variable laser shots (Fig. 2). It can be seen from Fig. 1 that even 1 laser shot with lowest laser beam energy (120 mJ, Fig. 1a) causes material ablation in some microareas, probably those where laser light was better absorbed. The higher laser beam energy (starting from 170 mJ, Fig. 1b) leads to material melting (characteristic rim appears around the heated areas) and partial ablation of molten material. With laser beam energy of 480 mJ, the rims formed by molten material surrounding heated microareas/dots integrate and form of continuous network (Fig. 1f). For further detailed investigation samples after PLIH with 120 mJ were chosen. Multiple heating leads not only to melting of the surface, but also causes material ablation (Fig. 3a, d). It is clearly seen for the sample after 50 laser shots (Fig. 3a). The number of laser shots over 100 led to the formation of ripples in single microareas (Fig. 3b, d). The ripples appeared with increasing numbers of incident laser shots. The distance measured between the ripples was equal to the wavelength of Nd:YAG laser beam (~1064 nm). According to Jia et al. [12] the ripples originate from the interference between the incident laser light and the scattered tangential wave, which appears as a result of incident laser light partial scattering by surface defects. As mentioned, the ripples appeared with increasing numbers of incident laser shots.

The careful TEM examination revealed several important characteristics of PILH processing. The laser heating led to the formation of fine-grained crystalline structure in the central parts of the microareas (Fig. 4a). The selected area electron diffraction (SAED) pattern indicated the presence α-Fe(Si) grains.

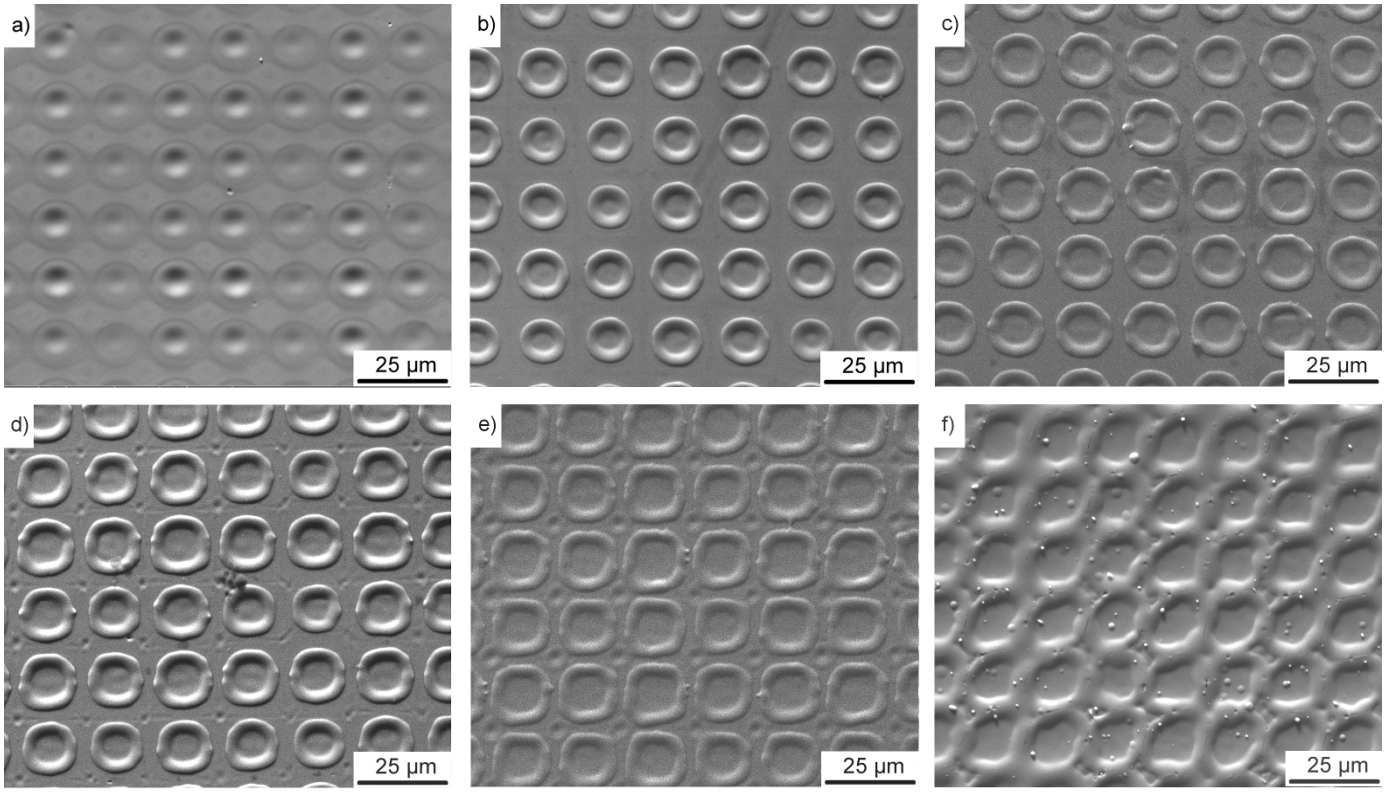

Fig. 1. SEM images of samples after heating with one laser shot with different laser beam energy: a – 120 mJ, b – 170 mJ, c – 230 mJ, d – 300 mJ, e – 360 mJ, f – 480 mJ

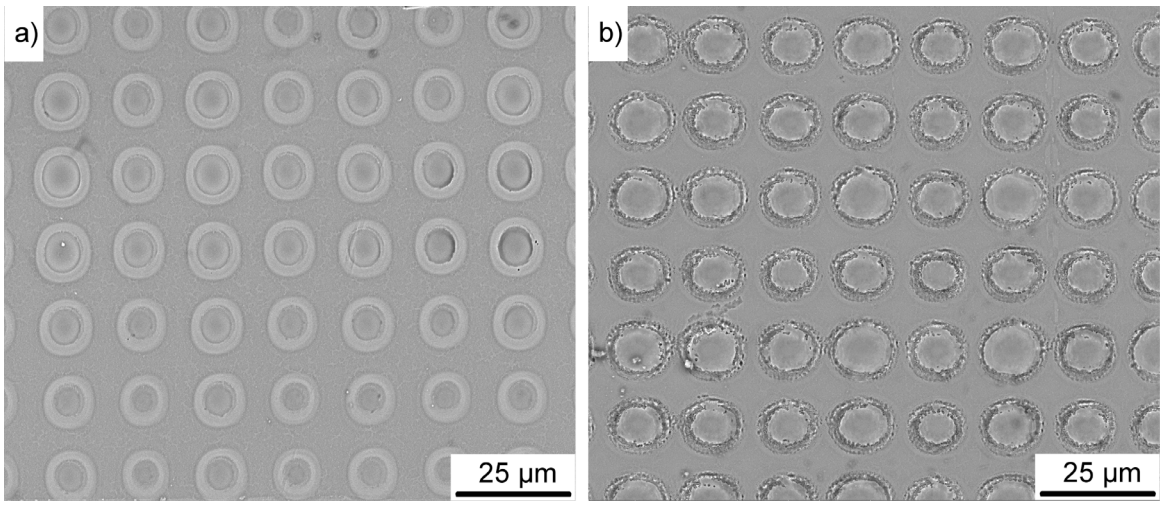

Fig. 2. SEM images of sample after PLIH with 120 mJ laser beam energy and variable number of shots: a – 50, b – 500

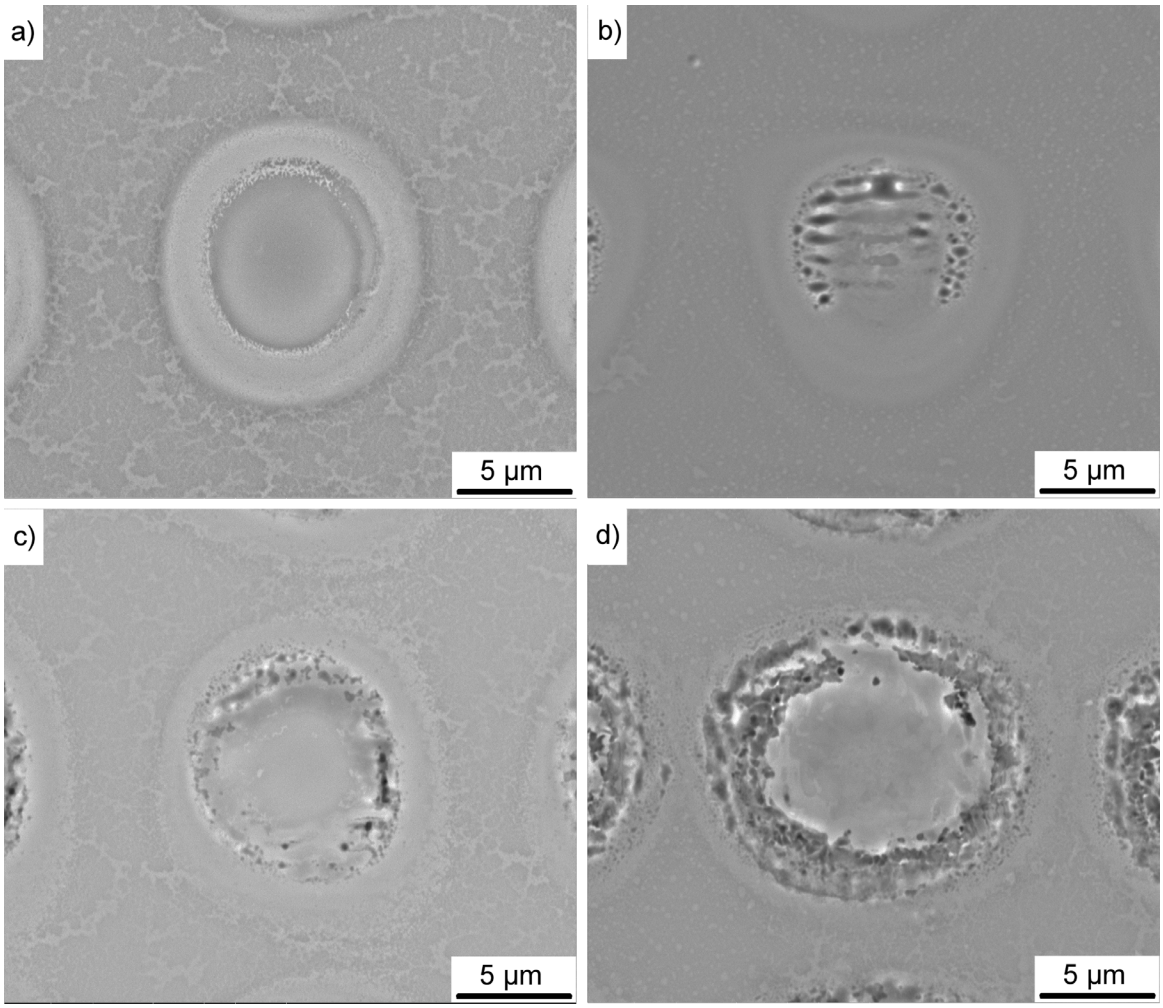

Fig. 3. Magnified SEM images of sample after PLIH with 120 mJ energy and variable number of shots: a – 50, b – 100, c – 300, d – 500

Peripherals are characterized by nanocrystals in an amorphous matrix (Fig. 4b). It should be emphasized that the laser beam has a Gaussian distribution of intensity, which results in inhomogeneous heating across the laser beam diameter. The grain growth in the area (grain size over 500 nm), located close to the melted/solid material boundary, is likely due to the intensive material heating caused by heat accumulation during consecutive 300 laser pulses. In most cases, the cold bulk of the material may be treated as semi-infinite which rapidly consumes thermal power input. In the presented study (30 µm thick, 25 mm wide ribbon) auto-cooling occurs, but is probably effective for the first 100 shots. With the increased number of laser shots, with heat ac-

cumulation, melting, material ablation and grain growth may occur in the central part of heated micro-areas. TEM indicated the presence of crystalline structure up to 350 nm (Fig. 5a) below the heated surface over the amorphous matrix (Fig. 5b). The SAED pattern from the sample cross-section show [001] oriented α-Fe(Si) grains (Fig. 5a). High resolution transmission electron microscopy revealed the presence of nanometric α-Fe(Si) crystals [001] oriented in an amorphous matrix (Fig. 6) in the heat affected zone, located to about 100 nm beneath the crystallization front, as presented in Fig. 5.

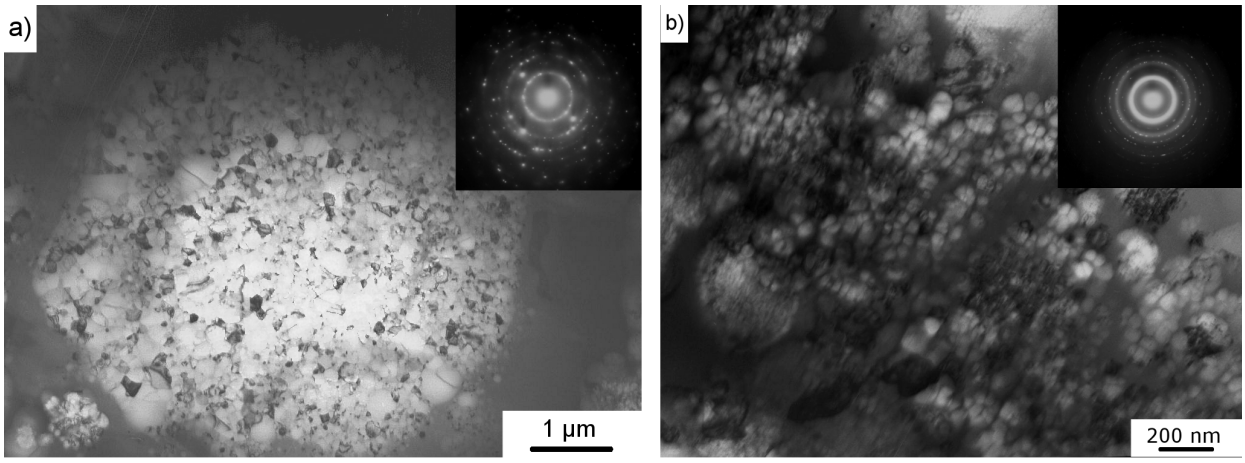

Fig. 4. TEM images from laser heated microarea – a, and heat affected zone of the laser beam – b

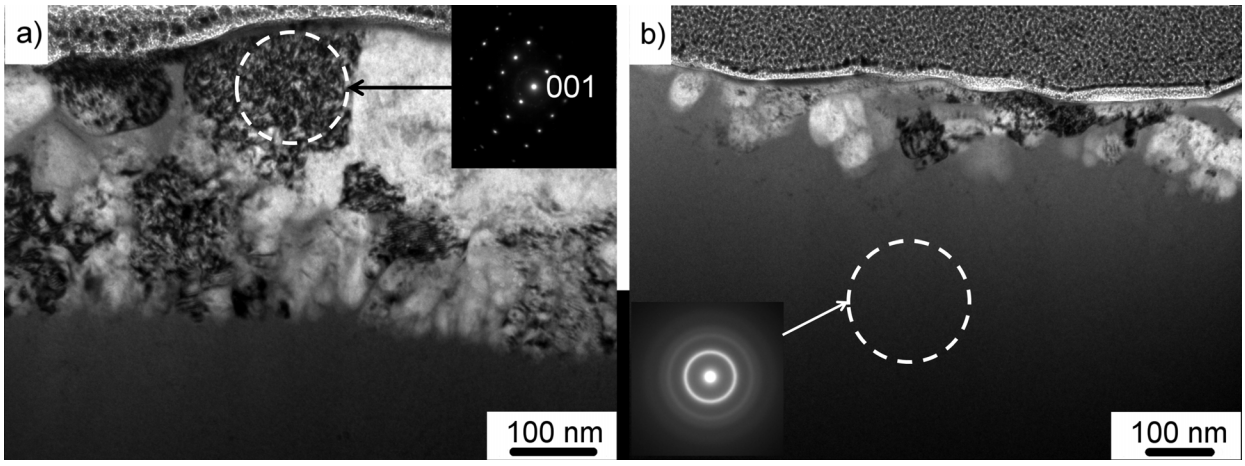

Fig. 5. TEM images of cross-section from laser heated microarea: a – centre of laser heated microarea, b – peripheral area

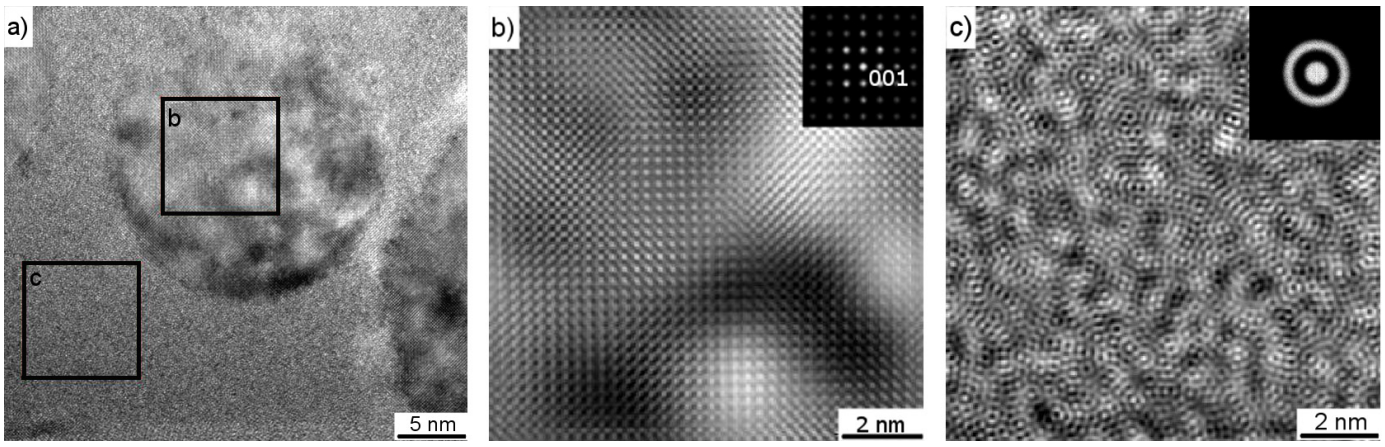

Fig. 6. HRTEM images of the zone heat affected by the laser beam: a – general view, with two marked areas (b and c); b – Fourier transform (FT) of the (001) diffraction spots in the area marked by the square (b) from Fe(Si)α nanocrystal, c – Fourier transform in the area marked by the square (c) shows amorphous matrix

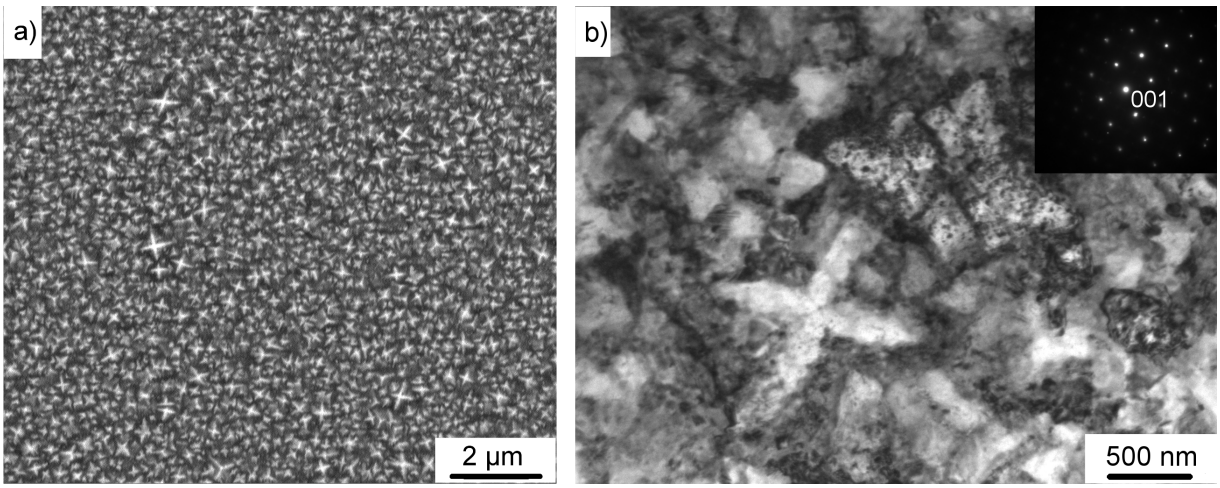

Fig. 7. Images of crystallized sample at 600°C a – SEM, b – TEM

Structure observations of the etched sample surface after conventional crystallization showed that the structure is composed of dendrites (Fig. 7a). TEM observations confirmed dendritic structure with varied dendrite size (Fig. 7b). The SAED pattern indicates the occurrence of [001] oriented α-Fe(Si) dendrites (Fig. 7b). The main difference between laser treatment and material after annealing is that, the PLIH produced the equiaxed fine-grain structure (Fig. 4), while conventional annealing led to the dendritic crystallization (Fig. 7). The dendritic crystal growth, observed during conventional annealing, resulted from a slower nucleation rate and relatively long time of annealing, Comparing to the PLIH, during which α-Fe(Si) nuclei have free space and long time to grow. In contrast, during PLIH, due to rapid heating and subsequent immediate rapid cooling, there is no enough time for nuclei growth. Indeed, with each subsequent laser shot the amorphous matrix saturates with ultra-fine equiaxed grains [13]. However, because of heat accumulation, occurring with higher number of the laser shots, the grain growth may occur.

3.2. Magnetic structure

The MFM reveals the magnetic structure of a material by detection its magnetization. The amorphous FeSiB is very soft magnetic material and did not give enough magnetic signal (Fig. 8) and the magnetic forces image is nearly the same as topography of the amorphous sample (Fig. 8). The PLIH with 120 mJ energy and 300 laser shots produced periodically placed crystallized areas, and MFM detected strong magnetic signal only in those areas (Fig. 9). This is because of the harder magnetic properties of crystalline than amorphous material. The sample after crystallization during conventional annealing was characterized by extended magnetic structure (Fig. 10). The crystallization deterioted soft magnetic properties and remanence as it was detected by MFM.

3.3. Magnetic properties

Magnetic hysteresis loop measurements of an amorphous sample proved soft magnetic properties of this material (Fig. 11).

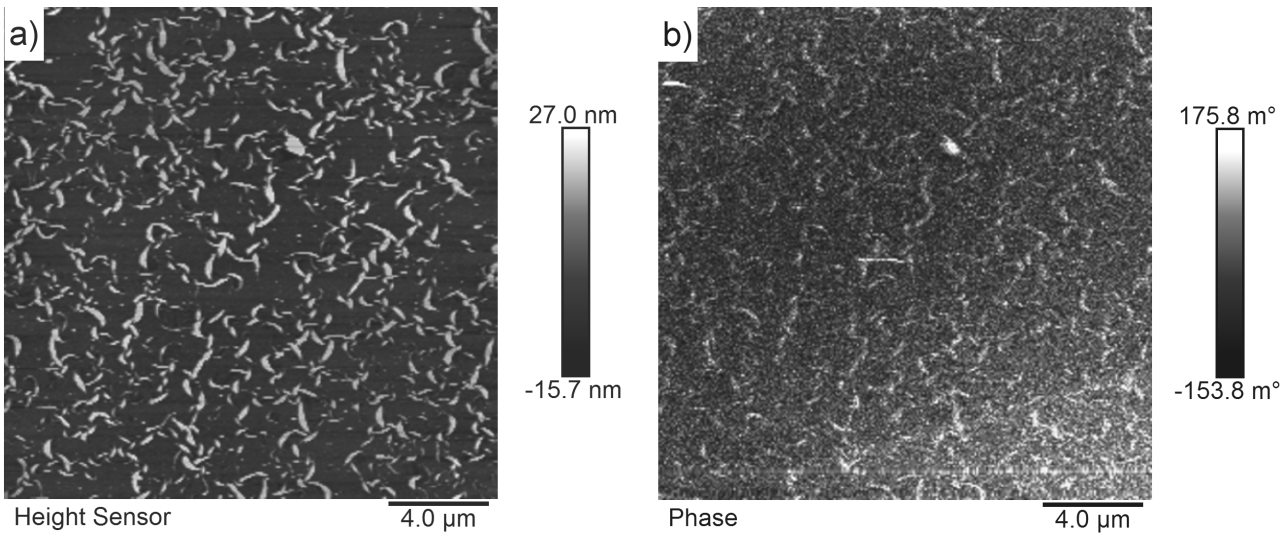

Fig. 8. Magnetic force microscopy images from amorphous material a – topography, b – magnetic forces

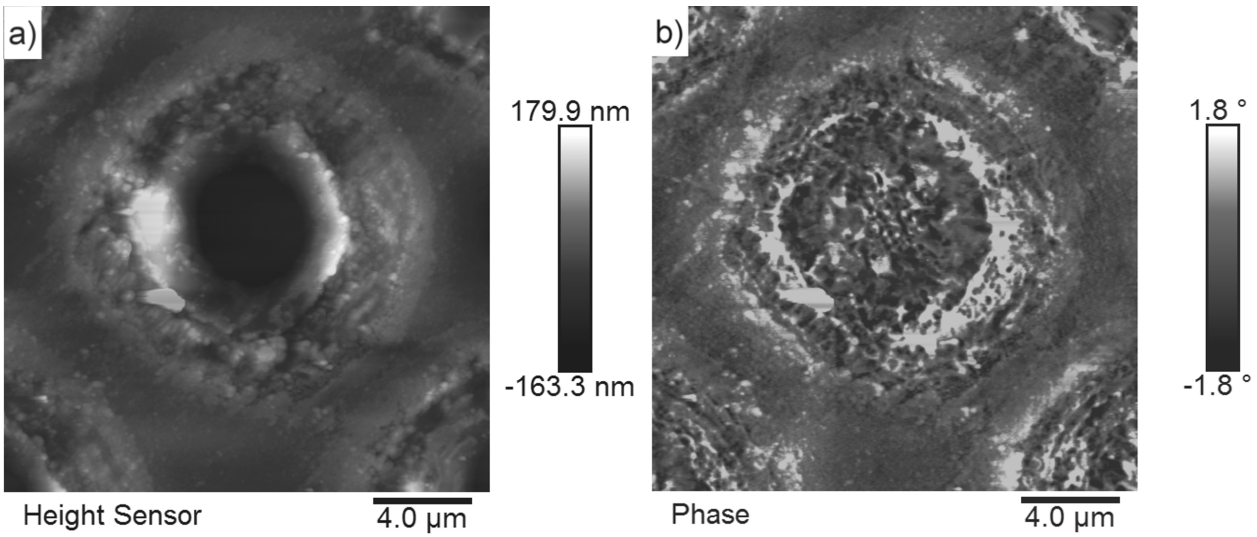

Fig. 9. Magnetic force microscopy images from a laser heated microarea a – topography, b – magnetic forces

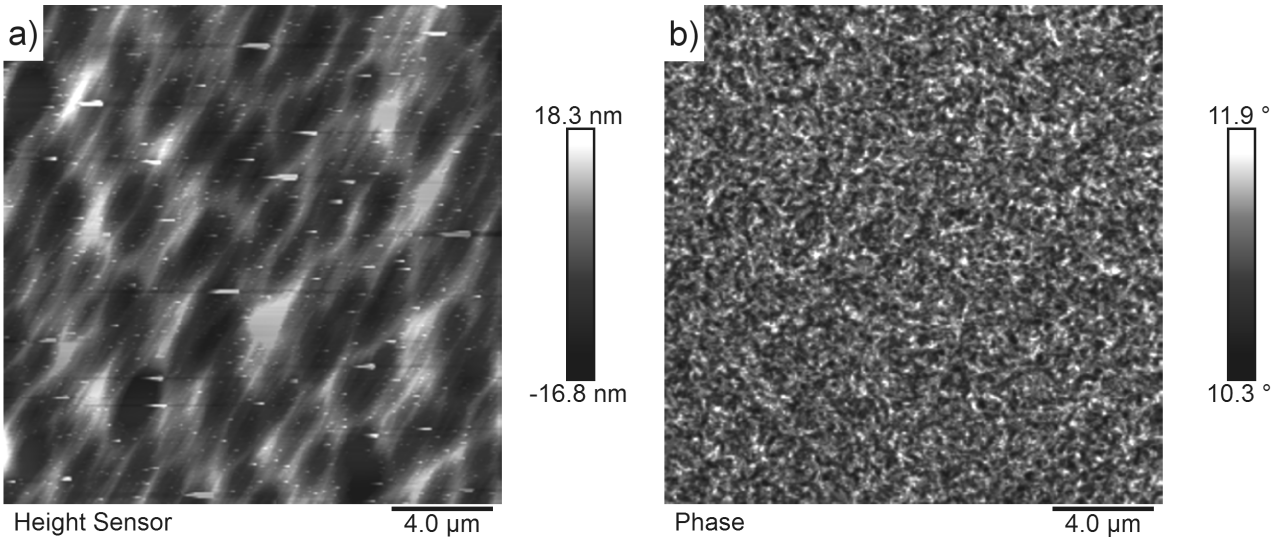

Fig. 10. Magnetic force microscopy images from annealed material at 600°C a – topography, b – magnetic forces

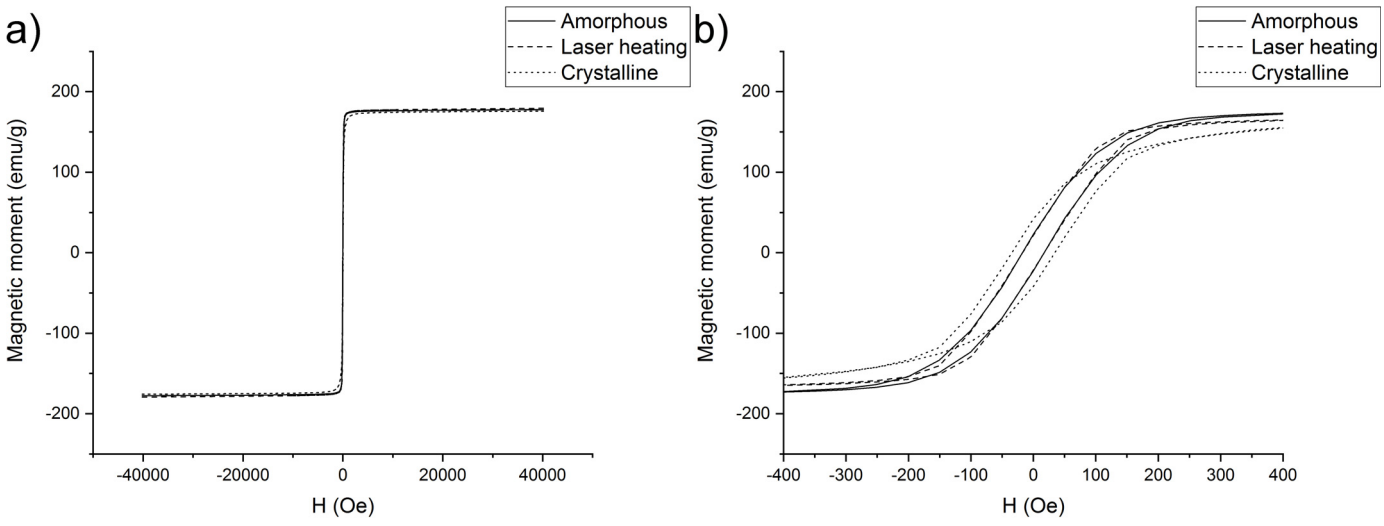

Fig. 11. Magnetic hysteresis loop measurement of amorphous, crystalline and laser heated samples a – full range measured scale b – magnification of coercivity field

The measured coercivity of amorphous ribbon was 20 Oe and the saturation magnetization was about 160 emu/g. Samples after laser irradiation with 120 mJ energy and 500 laser shots also were characterized by soft magnetic properties (Fig. 11). Coercivity for this sample was 18 Oe and saturation magnetization was about 170 emu/g. Measurements of crystalline material proved that crystallization occurring during conventional annealing deteriorated soft magnetic properties (Fig. 11). In such a case the coercivity was 40 Oe, but saturation magnetization was 150 emu/g.

4. Summary

The interference pulsed laser heating process applied to the FeSiB ribbons led to create periodically placed laser heated microareas (diameter of about 12-15 μm). The ultra-fine grain structure up to about 350 nm depth beneath the sample surface was produced only in laser heated microareas. Electron diffraction indicated the occurrence of crystalline structure of α-Fe(Si). Conventional annealing of FeSiB at 600°C is characterized by α-Fe(Si) dendritic structure. Differences of crystallization during laser treatment and annealing evidently gave new knowledge about forming microstructure Fe-based amorphous alloy.

Magnetic force microscopy revealed magnetization of laser heated microareas/dots. The amorphous matrix was characterized by near zero magnetic signal. The dendritic structure gave rise to the strong magnetic signal at all surfaces. This is the effect of higher remanence than in the amorphous material.

Magnetic hysteresis loop measurements indicated that the amorphous material had 20 Oe coercivity and 160 emu/g saturation magnetization. Laser heating decreased the coercivity by about 2 Oe and increased saturation magnetization by about 10 emu/g. Double coercion and saturation magnetization reduced at about 10 emu/g was effect of annealing at 600°C of FeSiB material.

Acknowledgement

The authors would like to acknowledge financial support from the National Science Centre (NCN) of Poland (contract number: OPUS 10, UMO-2015/19/B/ST8/01070).

REFERENCES

[1] J. Marczak, J. Kusiński, R. Major, A. Rycyk, A. Sarzyński, M. Strzelec, K. Czyz, Opt. Appl. **44** (2014). DOI:10.5277/oa140408.

[2] M. Gedvilas, S. Indrišiunas, B. Voisiat, E. Stankevičius, A. Selskis, G. Račiukaitis, Phys. Chem. Chem. Phys. **20** (2018). DOI:10.1039/c7cp08458g.

[3] R. Ostrowski, J. Kusiński, K. Czyż, A. Rycyk, A. Sarzyński, W. Skrzeczanowski, M. Strzelec, O. Czyż, Photonics Lett. Pol. **9** (2017). DOI:10.4302/plp.v9i3.762.

[4] L. Parellada-Monreal, I. Castro-Hurtado, M. Martínez-Calderón, A. Rodriguez, S.M. Olaizola, D. Gamarra, J. Lozano, G.G. Mandayo, Appl. Surf. Sci. **441** (2018). DOI:10.1016/j.apsusc.2018.02.031.

[5] Y. Yoshizawa, S. Oguma, K. Yamauchi, J. Appl. Phys. **64** (1988). DOI:10.1063/1.342149.

[6] G. Herzer, Handb. Magn. Mater. **10** (1997). DOI:10.1016/S1567-2719(97)10007-5.

[7] R. Nowosielski, R. Babilas, L. Ochin, Z. Stokłosa, Arch. Mater. Sci. Eng. **30** (2008).

[8] J.R. Greer, J.T.M. De Hosson, Prog. Mater. Sci. **56** (2011). DOI:10.1016/j.pmatsci.2011.01.005.

[9] A. Inoue, B. Shen, T. Ohsuna, Mater. Trans. **43** (2002). DOI:10.2320/matertrans.43.2337.

[10] S. Katakam, A. Devaraj, M. Bowden, S. Santhanakrishnan, C. Smith, R. V. Ramanujan, T. Suntharampillai, R. Banerjee, N.B. Dahotre, J. Appl. Phys. **114** (2013). DOI:10.1063/1.4829279.

[11] J. Kusiński, O. Czyż, A. Radziszewska, J. Morgiel, R. Ostrowski, M. Strzelec, K. Czyż, A. Rycyk, Arch. Foundry Eng. **18** (2018). DOI:10.24425/122497.

[12] W. Jia, Z. Peng, Z. Wang, X. Ni, C. yue Wang, Appl. Surf. Sci. **253** (2006). DOI:10.1016/j.apsusc.2006.02.003.